Cell Stem Cell
Article

Signaling through BMPR-IA Regulates Quiescence and Long-Term Activity of Neural Stem Cells in the Adult Hippocampus

Helena Mira,[1,2,10,*] Zoraida Andreu,[2,3,10] Hoonkyo Suh,[1,4] D. Chichung Lie,[5] Sebastian Jessberger,[1,6] Antonella Consiglio,[1,7] Juana San Emeterio,[2] Rafael Hortigüela,[2] María Ángeles Marqués-Torrejón,[3] Kinichi Nakashima,[1,8] Dilek Colak,[9] Magdalena Götz,[9] Isabel Fariñas,[3] and Fred H. Gage[1,*]

[1]Laboratory of Genetics, The Salk Institute for Biological Studies, La Jolla, CA 92037, USA
[2]Área de Biología Celular y Desarrollo, Centro Nacional de Microbiología, Instituto de Salud Carlos III, Majadahonda, 28220 Madrid, Spain
[3]Departament de Biologia Cellular, Universitat de València and CIBERNED, 46100 València, Spain
[4]Stem Cells and Regenerative Medicine, Lerner Research Institute, Cleveland Clinic, Cleveland, OH 44195, USA
[5]Institute for Developmental Genetics, Helmholtz Center Munich, German Research Center for Environmental Health, 85764 Munich-Neuherberg, Germany
[6]Institute of Cell Biology, Department of Biology, ETH Zurich, 8092 Zurich, Switzerland
[7]Centre de Medicina Regenerativa de Barcelona, 08003 Barcelona, Spain
[8]Laboratory of Molecular Neuroscience, Graduate School of Biological Sciences, Nara Institute of Science and Technology, 8916-5 Takayama, 630-0101 Ikoma, Japan
[9]Institute for Stem Cell Research, Helmholtz Center Munich, German Research Center for Environmental Health, 85764 Munich-Neuherberg, Germany
[10]These authors contributed equally to this work
*Correspondence: helena.mira@uv.es (H.M.), gage@salk.edu (F.H.G.)
DOI 10.1016/j.stem.2010.04.016

SUMMARY

Neural stem cells (NSCs) in the adult hippocampus divide infrequently, and the molecules that modulate their quiescence are largely unknown. Here, we show that bone morphogenetic protein (BMP) signaling is active in hippocampal NSCs, downstream of BMPR-IA. BMPs reversibly diminish proliferation of cultured NSCs while maintaining their undifferentiated state. In vivo, acute blockade of BMP signaling in the hippocampus by intracerebral infusion of Noggin first recruits quiescent NSCs into the cycle and increases neurogenesis; subsequently, it leads to decreased stem cell division and depletion of precursors and newborn neurons. Consistently, selective ablation of *Bmpr1a* in hippocampal NSCs, or inactivation of BMP canonical signaling in conditional *Smad4* knockout mice, transiently enhances proliferation but later leads to a reduced number of precursors, thereby limiting neuronal birth. BMPs are therefore required to balance NSC quiescence/proliferation and to prevent loss of the stem cell activity that supports continuous neurogenesis in the mature hippocampus.

INTRODUCTION

Quiescence of somatic stem cells is critically important for the maintenance of tissue-specific germinal reservoirs during adulthood. Stem cells from diverse adult compartments are depleted when forced to proliferate (Cheng et al., 2000; Kippin et al., 2005; Ruzankina et al., 2007), and quiescence may function as a protective mechanism that counteracts stem cell exhaustion. In the mature mammalian nervous system, adult neural stem cells (NSCs) generate new neurons throughout life, but there is little information regarding the molecules that regulate their relative quiescence. Adult NSCs are located in two specialized brain niches: the subependymal zone (SEZ), which lines the lateral ventricles, and the hippocampal subgranular zone (SGZ) apposed to the innermost layer of the dentate gyrus (reviewed by Temple and Alvarez-Buylla, 1999; Zhao et al., 2008). In the latter, undifferentiated cells expressing the Sry-related high mobility group (HMG) box transcription factor *Sox2* are the primary source for NSCs. On the basis of morphological criteria, on the expression of unique sets of cellular markers, and on lineage tracing, two types of lineage-related $SOX2^+$ stem/precursor cells that contribute neuronal progeny have been identified in the SGZ: (1) radial $SOX2^+$ cells, which bear a radial process spanning the granule cell layer and express NESTIN, the glutamate transporter GLAST, and the glial fibrillary acidic protein GFAP among other markers (also named rA cells or type 1 cells), and (2) nonradial $SOX2^+$ cells (or type 2a), which may arise from the radial cells and do not express GFAP. This distinction correlates with a different proliferation state of the cells, as $SOX2^+$ radial cells rarely divide whereas $SOX2^+$ nonradial cells appear to cycle relatively more often; consequently, it has been suggested that the radial cell population constitutes a stem cell reservoir (Seri et al., 2001, 2004; Filippov et al., 2003; Fukuda et al., 2003; Kronenberg et al., 2003; Suh et al., 2007).

Although the phenotypes of both radial and nonradial $SOX2^+$ cell types have been extensively characterized in numerous studies, our molecular understanding of their regulation is still very limited. In vivo cycling of the adult hippocampal $SOX2^+$

NSC population is relatively low, and most cells are held in a quiescent state. Indeed, in young transgenic mice harboring the green fluorescent protein (GFP) under the control of the murine *Sox2* promoter, less than 10% of the *Sox2*-GFP$^+$ cells in the SGZ colabel with cell proliferation markers (Suh et al., 2007). As rodents grow old (Hattiangady and Shetty, 2008; Aizawa et al., 2009), SOX2$^+$ cells lose proliferative capacity, suggesting that adult NSCs may have a finite number of cycles. This finding points to a role for quiescence in the maintenance of the regenerative potential of the hippocampal dentate gyrus. However, how quiescence of SOX2$^+$ stem cells is governed during adulthood is still an unresolved question.

Among the signaling pathways that govern stem cells across phylogeny, bone morphogenetic proteins (BMPs) have emerged as critical regulators of stem cell self-renewing divisions and maintenance in a wide variety of niches (reviewed by Varga and Wrana, 2005; Morrison and Spradling, 2008). BMPs belong to the TGF-β superfamily of cytokines and are pleiotropic molecules that exert a plethora of effects in the nervous system, ranging from dorsoventral patterning of the embryonic neural tube to proliferation, apoptosis, neurogenesis, and gliogenesis (reviewed by Panchision and McKay, 2002; Hall and Miller, 2004; Chen and Panchision, 2007). In the adult brain environment, the contribution of BMP signaling to stem cell regulation remains largely unexplored, although recently it has been suggested that the BMP pathway may have a central role in modulating NSC function (Lim et al., 2000; Coskun et al., 2001; Colak et al., 2008; Bonaguidi et al., 2008).

Here, we test the requirement of endogenous BMP signaling for the regulation of hippocampal NSCs. Both genetic deletion of *Bmpr1a* and *Smad4* in adult NSCs and infusion of the BMP antagonist Noggin show that canonical signaling downstream of the BMP type IA receptor is a key mediator of quiescence in adult NSCs. We evaluate BMP function both in vitro and in vivo and conclude that BMPR-IA is essential in regulating the equilibrium between stem cell proliferation and quiescence in the SGZ, preventing the premature depletion of NSC activity in the mature hippocampus.

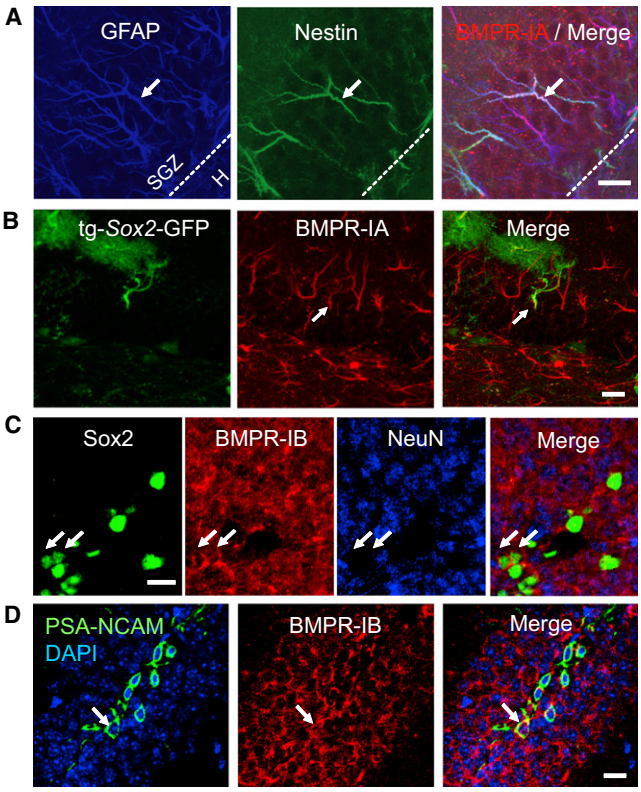

Figure 1. Adult Hippocampal Radial Stem Cells Express BMPR-IA

(A) Confocal microscopy images of adult hippocampal mouse sections showing GFAP (blue), NESTIN (green), and BMPR-IA (red) triple-labeled processes (arrow) of NSCs projecting radially from the SGZ (dotted line). See also Figure S1 for additional data. The scale bar represents 20 μm.

(B) Section from an adult tg-*Sox2*-GFP mouse. Arrow points to a radial stem cell process (immunoreactive for GFP, green) labeled for BMPR-IA (red). The scale bar represents 20 μm.

(C) BMPR-IB staining was detected in NeuN$^+$ granule neurons located in the granule cell layer and in some SOX2$^+$ cells (arrows) located in the SGZ. The scale bar represents 10 μm.

(D) Immature neurons expressing PSA-NCAM also stained for BMPR-IB. The scale bar represents 20 μm. H, hilus. See scheme in Figure S7.

RESULTS

BMPR-IA Is Expressed by Adult Hippocampal Radial NSCs

BMP ligands signal through a tetrameric complex formed by the BMP type II receptor (BMPR-II) and different classes of BMP type I receptors, the prototypic ones being BMPR-IA (ALK3) and BMPR-IB (ALK6). Expression of *Bmpr-II* had been previously documented in the hippocampus by in situ hybridization (Söderström et al., 1996; Charytoniuk et al., 2000), so we analyzed type I receptor expression by immunostaining. We found that radial stem cells coexpressing GFAP and NESTIN were frequently stained for BMPR-IA (Figure 1A). Consistently, BMPR-IA signal was detected in GFP$^+$ radial cells from transgenic mice expressing the GFP reporter under the regulation of the *Sox2* promoter (Figure 1B). In addition, the vast majority of GFAP$^+$ astrocytes in the dentate gyrus and the hilar region were immunoreactive for BMPR-IA (Figure 1A and Figure S1, available online). In marked contrast, BMPR-IB expression was mostly confined to the neuronal population, given that NeuN$^+$ mature neurons and PSA-NCAM$^+$ immature neurons stained for BMPR-IB (Figures 1C and 1D). Some nonradial cells that formed clusters in the SGZ expressed low levels of SOX2 and were also immunoreactive for BMPR-IB (Figure 1C). Altogether, these findings suggested that BMPR-IA might regulate an early event in adult neurogenesis, whereas BMPR-IB might have a later role, during neuronal differentiation.

Canonical BMP Signaling in the Adult Hippocampus Is Active in Nondividing SGZ Cells

The interaction of BMPs with their receptors can trigger several pathways, including the "canonical" Smad-mediated pathway, in which activated BMPR-I phosphorylates the DNA binding proteins SMAD1/5/8, causing their nuclear translocation. Immunostaining with anti-phospho-SMAD1 (Ser463/465) was assessed in adult animals that were briefly pulsed with the S-phase marker 5-bromodeoxyuridine (BrdU). P-SMAD1 staining revealed that canonical BMP signaling is active in the majority of radial and

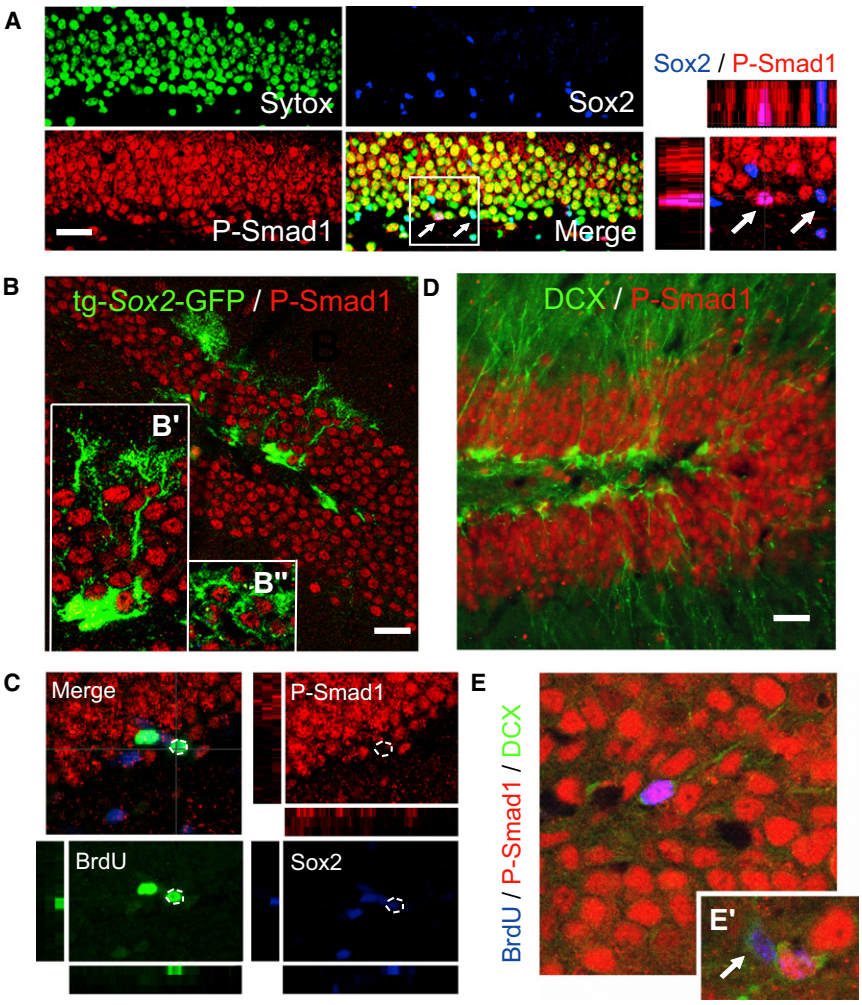

Figure 2. BMP Signaling Is Active in Adult Hippocampal Stem/Precursor Cells that Are Not Cycling

(A) Confocal microscopy images of adult hippocampal mouse sections showing that most SOX2$^+$ cells (blue) in the SGZ are immunoreactive for P-SMAD1 (red) in their nucleus (green; fraction of SOX2$^+$ cells that were P-SMAD1$^+$: 64% ± 1%, average ± SEM, n = 2). Of these, ~70% displayed medium to high signal level. Confocal 3D reconstruction of the boxed area, showing colocalization of phosphorylated SMAD1 and SOX2 proteins in some SGZ nuclei (left arrow), is shown on the right. Top shows the *x-z* plane; left shows the *y-z* plane. The scale bar represents 40 μm.

(B) Image of a section from a tg-*Sox2*-GFP transgenic mouse showing the P-SMAD1$^+$ nucleus of radial (B′) and nonradial (B″) *Sox2*-expressing NSCs (immunoreactive for GFP, green). The scale bar represents 40 μm.

(C) Section from an adult animal pulsed with BrdU (four injections every 2 hr) and euthanized 1 hr later. The immunostaining and the confocal analysis shows SOX2$^+$ cells that incorporated BrdU and were negative for P-SMAD1 (dotted circles).

(D) Most DCX$^+$ immature neurons (green) in the SGZ stained for P-SMAD1. Note that nuclei of densely packed mature neurons located in the granule layer were also immunoreactive for P-SMAD1. The scale bar represents 40 μm.

(E) Detail from a section of an adult animal labeled with BrdU, showing a newborn neuron (DCX$^+$BrdU$^+$) that stained for P-SMAD1 apparently migrating into the granule layer. As shown in (E′), we could observe some newborn neurons with poor dendritic processes that did not stain for P-SMAD1 (arrow). See also Figure S2 for additional data. See scheme in Figure S7.

nonradial SOX2$^+$ cells (Figures 2A and 2B), but the pathway is preferentially inactive in the few cells that have entered a new round of cell division (most SOX2$^+$ cells that incorporated BrdU were negative for P-SMAD1: 92% ± 8%, average ± SEM, Figure 2C). In addition, the majority of the doublecortin-positive (DCX$^+$) and NEUROD1$^+$ immature neurons/neuroblasts stained for P-SMAD1 (Figure 2D and Figure S2). When adult animals were pulsed with BrdU for 3 days for labeling and tracking newborn cells, we observed that most of the DCX$^+$BrdU$^+$ newly generated neurons that were extending dendritic processes toward the molecular layer were P-SMAD1$^+$ (Figure 2E); however, we also found some more immature DCX$^+$BrdU$^+$ cells positioned along the SGZ, with shorter dendrites, that were negative for P-SMAD1 (Figure 2E′), suggesting that canonical signaling becomes reactivated in the neuronal progeny shortly after its commitment. Together, our results indicated that BMP signaling is inactive in most proliferating SGZ cells, whereas it is active in nondividing cells, including the quiescent SOX2$^+$ NSC population and the differentiated neurons.

BMP2/4 Trigger Canonical Signaling in Adult Hippocampal NSC Cultures Expressing BMPR-IA

We next examined the role of BMP signaling in adult hippocampus-derived NSCs (AH-NSCs) that can mimic the initial events of neurogenesis under proliferating conditions. Immunostaining and RT-PCR analysis revealed that AH-NSCs expressed *Bmpr1a* and *Bmpr2*, whereas *Bmpr1b* expression was only detected at very weak levels (Figures 3A and 3B). Of note, *Bmpr1a* expression was decreased, whereas *Bmpr1b* expression was progressively increased upon neuronal differentiation of AH-NSCs (Figure S3). Given that BMPR-IA preferentially binds ligands from the Dpp class (BMP2/4) as opposed to the 60A class (BMP5-8) (ten Dijke et al., 1994), we challenged AH-NSCs with the purified recombinant BMP2 and BMP4 proteins. BMP2/4 triggered phosphorylation and nuclear translocation of SMAD1 (Figures 3C and 3D) and upregulated the expression of several SMAD targets, such as *Id1-4*, *Hes1*, or the inhibitory *Smad6/7* genes (Figures 3E and 3F), showing that AH-NSCs responded to BMPs through activation of the canonical pathway.

BMP2/4 Treatment Decreases Proliferation and Increases Quiescence of AH-NSC Cultures

We assayed for proliferation effects of BMPs in AH-NSCs grown under self-renewing conditions in the presence of fibroblast growth factor 2 (FGF2). Under mitogenic stimulation, exposure to increasing BMP2 doses markedly decreased the percentage of cells that incorporated BrdU ($p < 0.05$, Figures 4A and 4B).

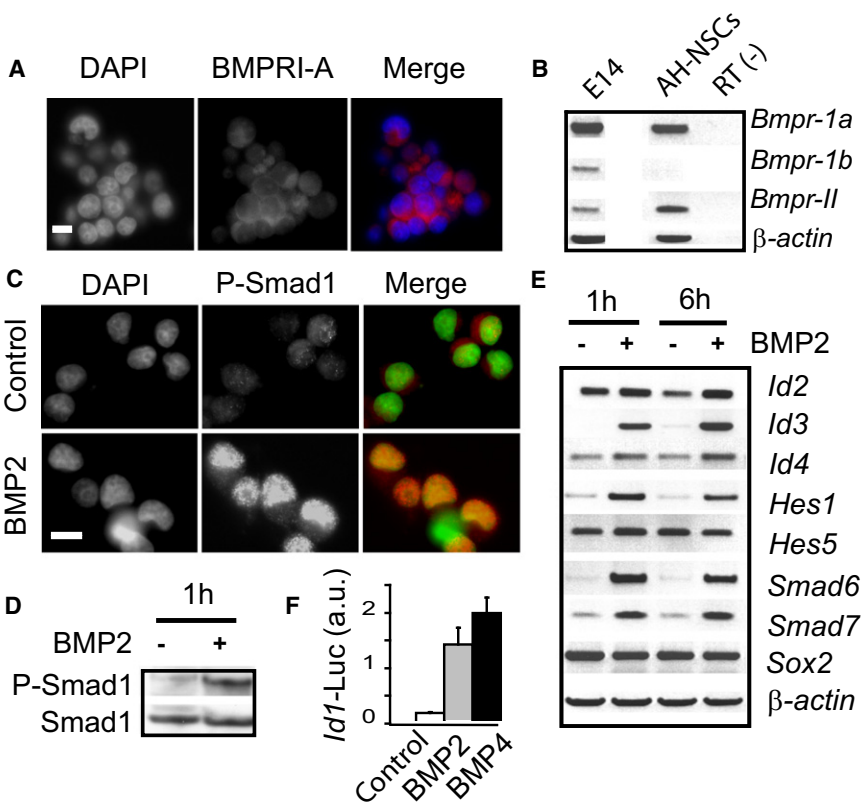

Figure 3. BMP Treatment Activates Canonical Signaling in AH-NSC Cultures Expressing BMPR-IA

(A) Immunofluorescent microscopy image showing BMPR-IA signal in AH-NSCs, growing in the presence of FGF2. The scale bar represents 10 μm.

(B) *Bmpr-1a* and *Bmpr-II* are expressed in proliferating AH-NSC cultures, as detected by RT-PCR. *Bmpr-1b* expression is low (average threshold cycle calculated by real-time quantitative RT-PCR [Cp ± SEM]: 28.4 ± 0.3 for *Bmpr-1a* and 31.0 ± 0.1 for *Bmpr-1b*). See also Figure S3 for additional data.

(C) Immunofluorescent analysis of BMP2-treated and untreated AH-NSCs, showing activation of canonical BMP signaling through increased phosphorylation and nuclear translocation of SMAD1. The scale bar represents 10 μm.

(D) Western blot analysis of protein extracts from BMP2-treated and untreated AH-NSCs corroborating the activation of canonical signaling through phosphorylation of SMAD1.

(E) mRNA expression of several SMAD target genes by RT-PCR.

(F) Relative luciferase activity in AH-NSCs electroporated with *Id1*-reporter construct upon BMP2/BMP4 stimulation.

Consistently, cell cycle analysis by flow cytometry indicated that BMP treatment increased the proportion of cells in G_0/G_1 while decreasing the proportion of AH-NSCs in S phase and G_2/M phases (Figure S4). The decrease in proliferation was not due to cell death (propidium iodide labeled cells by flow cytometry: 1.26% ± 0.43% in FGF2 versus 0.95% ± 0.06% in FGF2+BMP4, p = 0.28) or to differentiation, given that the expression of the NSC marker SOX2 was maintained in the culture (Figure 4A). Rather, BMP appeared to antagonize the proliferative function of FGF2 because increasing the amount of mitogen in the medium partially blocked the dose-dependent effect of the BMP treatment on proliferation (Figure S5; Pera et al., 2003).

We next explored whether BMP treatment increased the quiescent (G_0-arrested) cell fraction. Given that G_0 cells are in a lower metabolic state and do not require robust RNA transcription, they can be identified by a 2N DNA content and a low level of RNA, with Hoechst 33342 and the Pyronin Y RNA dye. Two-parameter flow cytometry showed that the fraction of G_0 cells increased an average fold of 1.8 ± 0.2 after BMP exposure (n = 3, Figure S4). Moreover, when the BMP-treated FACS-sorted G_0 cells were challenged with the BMP antagonist Noggin, 81.3% ± 10.7% of the cells were NESTIN$^+$ (not shown) and 21.6% ± 7.8% of the cells started dividing after 24–48 hr (Figure S4). This finding indicated that the majority of the BMP-treated G_0 cells maintained stem/precursor properties and could re-enter the cell cycle. Thus, Noggin reverted the G_0 arrest induced by BMP signaling on AH-NSCs.

To test whether culture conditions such as cell density and adhesion influenced BMP functions, we also assayed for the effects of BMPs on AH-NSCs seeded at a very low density (0.5 cells/μL) and maintained as clonal floating aggregates termed neurospheres. Comparable numbers of spheres were formed in control medium with FGF2 or in medium containing FGF2 and 50 ng/mL BMP2/4 (331.67 ± 49.14 spheres in FGF2 versus 323.50 ± 83.19 spheres in FGF2+BMP4, p = 0.46, Figure 4C). We evaluated the proportion of cells per sphere that were in the cell cycle, using an antibody directed against Ki67, a protein that is present during all active phases of the cell cycle but is absent from resting (G_0) cells. The percentage of Ki67$^+$ cells was markedly diminished in the presence of BMP4 (p < 0.05, Figures 4E and 4F), and accordingly, the average diameter of the spheres was significantly decreased (p < 0.05, Figures 4C and 4D). Consistent with our previous results, cell death was unaffected (percentage of Caspase3$^+$ cells per sphere: 0.64% ± 0.46% in FGF2 versus 1.22 ± 0.3% in FGF2+BMP4, p = 0.29), and the proportion of cells that were NESTIN$^+$ or SOX2$^+$ did not change (Figure 4E, percentage of NESTIN$^+$ cells per neurosphere: 83.65% ± 3.74% in FGF2 versus 97.72% ± 1.85% in FGF2+BMP4; percentage of SOX2$^+$ cells: 89.27% ± 0.64% in FGF2 versus 92.6 ± 0.57% in FGF2+BMP4). In addition, >80% of the Ki67$^-$ cells were immunoreactive for NESTIN and SOX2, indicating that, at early time points, most G_0 (Ki67$^-$) cells were undifferentiated/immature and not terminally differentiated cells (Figure S5). Nevertheless, ~20% of the Ki67$^-$ cells expressed differentiation markers of the oligodendroglial or astroglial lineage, but no significant differences were found between control and BMP-treated neurospheres.

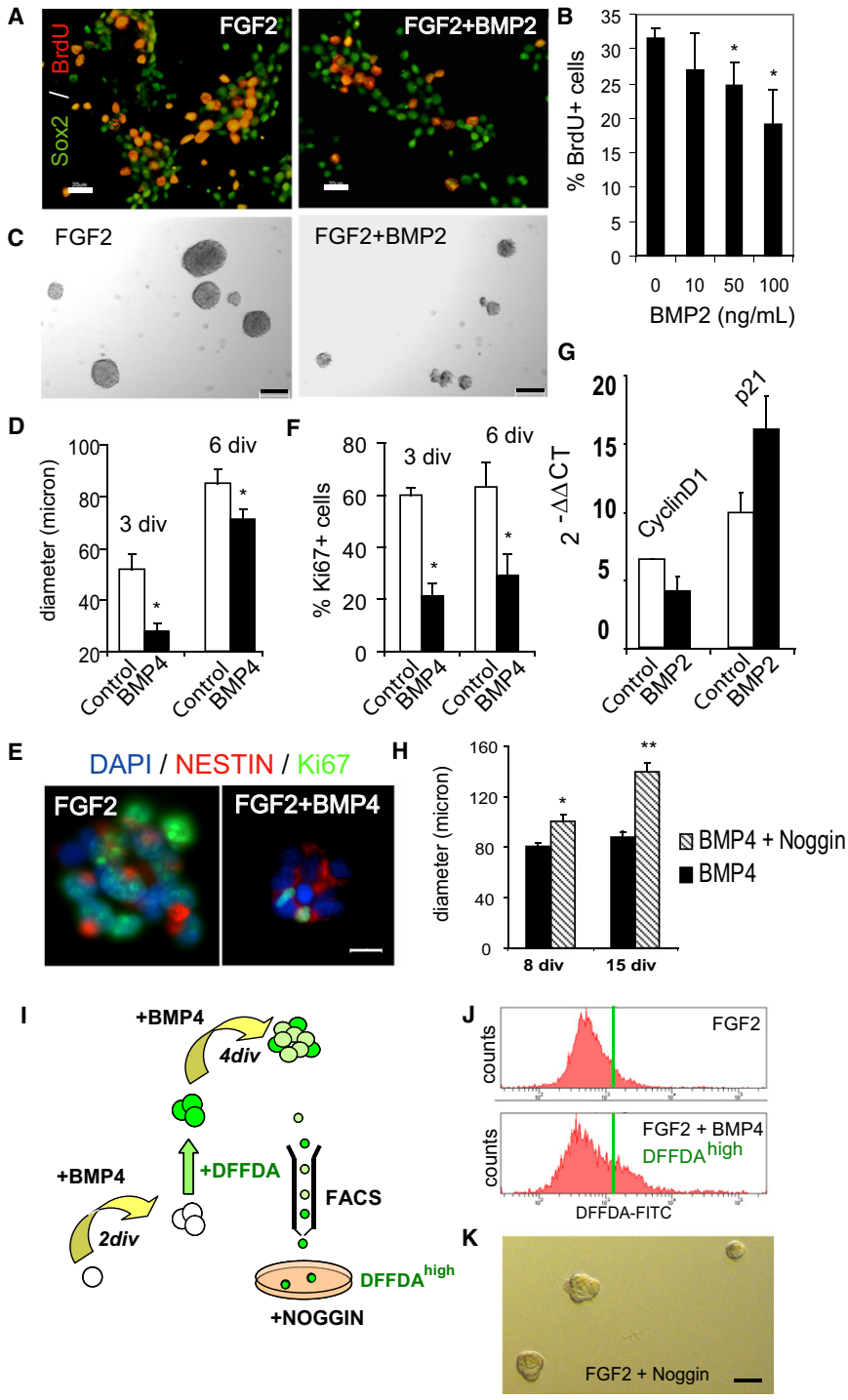

Figure 4. BMP Treatment Decreases Proliferation and Increases Quiescence of AH-NSC Cultures

(A) Immunofluorescent analysis of BMP-treated or untreated proliferating cells fixed at 2 days in vitro. BMP2 decreases the proportion of cells that are in S-phase ($BrdU^+$, red) while maintaining the expression of the NSC marker SOX2 (green). Scale bars represent 20 μm.

(B) Quantitative analysis showing that increasing concentrations of BMP2 decrease the percentage of $BrdU^+$ cells in AH-NSC cultures grown in proliferating medium with FGF2 (n = 3).

(C) Bright-field images of adult hippocampal neurospheres grown for 6 days in vitro. Note that approximately equal numbers of neurospheres are generated in the presence or absence of BMP2; however, the decrease in sphere size in BMP2-treated cultures is apparent. The scale bar represents 100 μm.

(D) A plot of the diameter of spheres that were generated after plating AH-NSCs in nonadherent conditions at very low density (250 viable cells per cm^2, n = 3).

(E) Immunofluorescent analysis of BMP-treated or untreated neurospheres fixed at 3 days in vitro. BMP4 decreases the proportion of cells that are in the cell cycle ($Ki67^+$, green) while maintaining the expression of the NSC marker NESTIN (red). The scale bar represents 10 μm.

(F) BMP4 treatment decreases the percentage of $Ki67^+$ cells per neurosphere (n = 3).

(G) qRT-PCR analysis showing decreased *CyclinD1* and increased $p21^{cip1/waf1}$ expression 4 days after BMP2 treatment of adult hippocampal sphere cultures (n = 2).

(H) The addition of Noggin (250 ng/mL) at day 6 progressively rescues the proliferating activity (size) of the BMP-treated spheres, as measured at days 8 and 15.

(I) Diagram depicting the experimental design employed to purify DFFDA-retaining cells from BMP4-treated neurospheres.

(J) Cytometry plot showing that BMP4 treatment increased the percentage of $DFFDA^{high}$ cells from 11% to 27%.

(K) Bright-field image of purified BMP4-treated $DFFDA^{high}$ cells plated in FGF2 + Noggin (100 ng/mL), showing secondary sphere formation after 48 hr. Paired Student's t test relative to control condition: *p < 0.05, **p < 0.01. The scale bar represents 20 mm. See also Figures S4 and S5 for additional data.

The decreased proliferation and increased G_0 cell fraction after BMP exposure correlated with the upregulation of the cell cycle inhibitor *Cdkn1a* ($p21^{Cip1/Waf1}$) and the downregulation of *CyclinD1* (Figure 4G). In addition, Noggin treatment in the presence of FGF2 presumably antagonized endogenous BMP effects by increasing the average sphere number (126% ± 4%) and diameter (187% ± 27%) and the percentage of $Ki67^+$ cells (120% ± 9%). Moreover, in agreement with a previous report (Bonaguidi et al., 2008), Noggin enhanced the net expansion of hippocampal sphere cultures that were serially passaged over 1 month in the presence of FGF2 but was not sufficient to promote proliferation of AH-NSCs (Figure S5).

At the level of clone size, the antiproliferative effect of BMP signaling could be reversed when BMP was replaced with

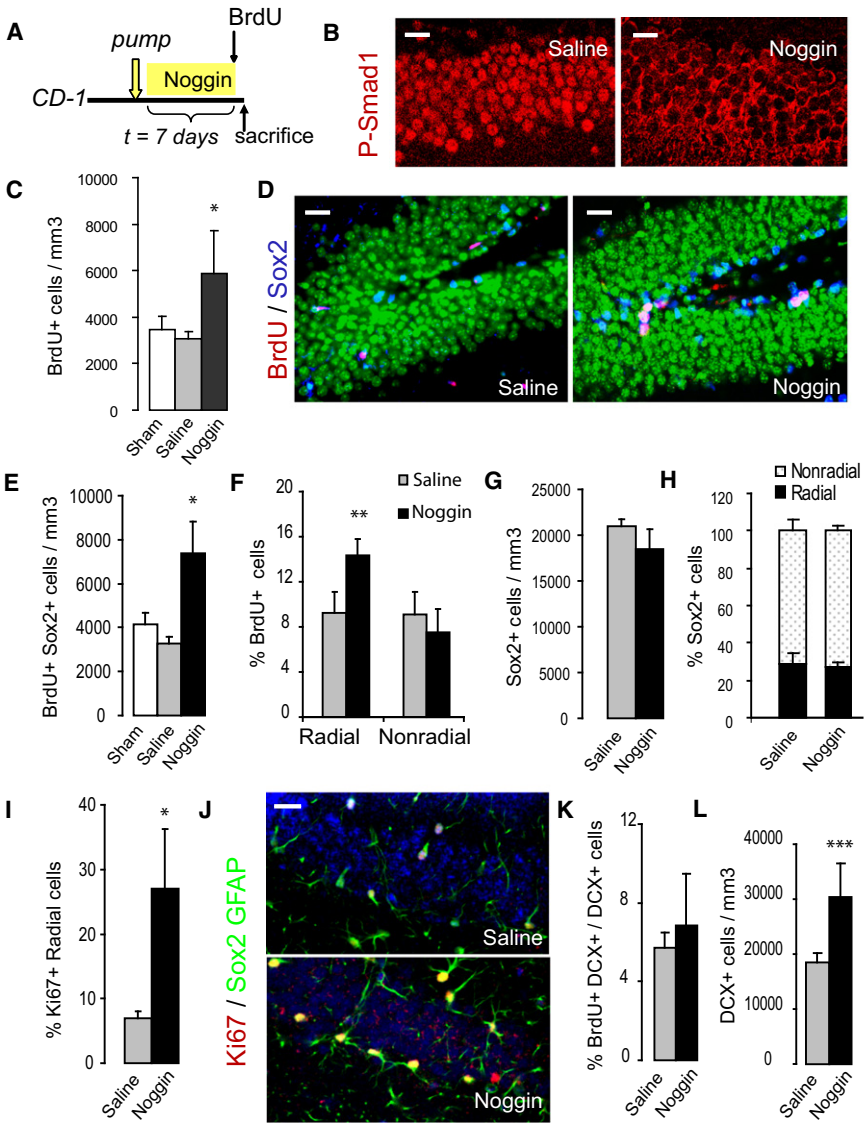

Figure 5. In Vivo Infusion of Noggin Increases Proliferation of SOX2$^+$ Radial NSCs

(A) Diagram depicting the experimental design employed. BrdU (seven injections every 2 hours) was administered prior to euthanasia.

(B) P-SMAD1 immunostaining in hippocampal sections from saline- and Noggin-infused mice. Note that nuclear localization of P-SMAD1 is abolished after Noggin exposure, demonstrating that the treatment was effective. Scale bars represent 20 μm.

(C) Quantitative analysis showing that 1 week of Noggin infusion enhanced cell proliferation in the hippocampus. Proliferation was calculated by the number of cells that incorporated BrdU per volume of granule cell layer.

(D) Confocal microscopy images of adult hippocampal mouse sections showing the increase in proliferative NSCs double labeled for SOX2 (blue) and BrdU (red). Nuclei were stained with Sytox-Green. Scale bars represent 40 μm.

(E) Immediately after 1 week of Noggin delivery, the number of SOX2$^+$ cells in S-phase increased.

(F) The percentage of radial cells (immunoreactive for SOX2 and GFAP) that incorporated BrdU increased; the proportion of nonradial cells (immunoreactive for SOX2 but not for GFAP) that incorporated BrdU did not change.

(G) The total number of SOX2$^+$ cells per volume of granule cell layer remained constant.

(H) The relative amount of radial and nonradial cells was maintained.

(I) Noggin increased the percentage of radial SOX2$^+$ cells that are in the cell cycle (Ki67$^+$).

(J) Confocal image showing that Noggin increased cell cycle entry of the radial NSC population. The scale bar represents 40 μm.

(K and L) The rate of proliferation of doublecortin-expressing (DCX$^+$) neuroblasts did not change (K), although as shown in (L), the total number of DCX$^+$ immature neurons augmented. Unpaired Student's t test: *$p < 0.05$, **$p < 0.01$, and ***$p < 0.001$.

Noggin (see the recovery of sphere diameters, Figure 4H). We confirmed this reversibility at the cellular level, by using the cytoplasmic retention dye carboxy-DFFDA, which is subject to dilution upon cell division. As illustrated in Figure 4I, we loaded spheres that were growing for 2 days with DFFDA, and we allowed them to grow for 4 additional days in FGF2+BMP4. Addition of BMP4 clearly increased (~2.5-fold) the DFFDA^{high} cell fraction (nondividing cells) relative to the control condition (Figure 4J). When BMP-treated DFFDA^{high} cells were FACS sorted and were placed at low density in FGF2 + Noggin medium, 46% ± 20% of the cells re-entered the cell cycle (were Ki67$^+$) and 35% ± 16% formed secondary clones (Figure 4K). These results collectively indicated that BMPs counteract the mitogenic stimulation of AH-NSCs by promoting the entry of the cells into quiescence. The contribution of other BMP signaling effects (i.e., cell cycle lengthening effects) to the decrease in proliferation cannot be excluded and remain to be explored.

BMP Signaling Regulates the Balance between AH-NSC Proliferation and Quiescence In Vivo

To assess the possibility that endogenous BMPs can regulate proliferation of NSCs in the hippocampal niche, we delivered Noggin into the lateral ventricle of the adult mouse brain. Animals were infused over 1 week and, on the last day of infusion, dividing cells were labeled with BrdU (Figure 5A). Acute delivery of Noggin efficiently blocked BMP canonical signaling in the hippocampus (Figure 5B) and increased the number of BrdU$^+$ cells in the SGZ (3073 ± 283 in saline [n = 8] versus 5868 ± 1853 in Noggin [n = 4], $p < 0.05$, Figure 5C).

Noggin infusion enhanced by 2-fold the percentage of SOX2$^+$ cells that were in S phase ($p < 0.05$, Figure 5D and 5E) but did not influence the total number of SOX2$^+$ cells in the SGZ ($p = 0.335$, Figure 5G) or the relative proportion of radial and nonradial cells (Figure 5H), suggesting that SOX2$^+$ cells divided asymmetrically. Interestingly, Noggin preferentially increased the proliferation of the GFAP$^+$SOX2$^+$ radial stem cell population ($p < 0.01$,

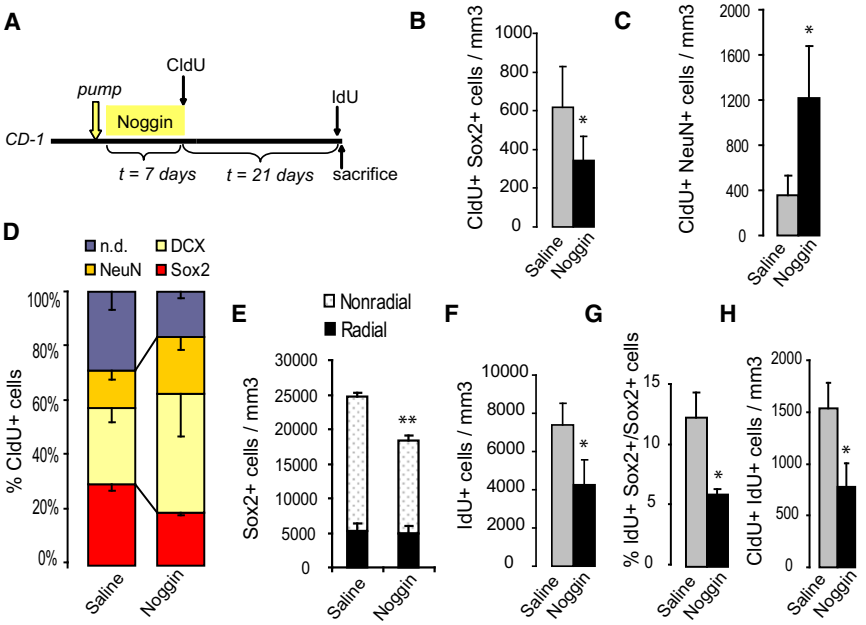

Figure 6. Noggin Infusion Leads in the Long Run to a Decrease in the Proliferative Activity of SOX2$^+$ Cells and of Label-Retaining NSCs

(A) Diagram depicting the experimental design for Noggin infusion and for the administration of CldU and IdU.

(B) Quantitative analysis showing that the number of SOX2$^+$ cells that retain the proliferative label CldU per volume of granule cell layer is decreased 3 weeks after pump removal.

(C) The number of NeuN$^+$ mature granule neurons marked with CldU is increased.

(D) The percentage of CldU$^+$ cells that stained for immature (DCX) and mature (NeuN) neuronal markers is increased at the expense of SOX2$^+$ cells. (n.d., not determined).

(E) The total number of SOX2$^+$ cells and the number of SOX2$^+$ nonradial cells per volume of granule cell layer decayed.

(F) Noggin exposure resulted 3 weeks later in decreased hippocampal proliferation (decreased number of IdU$^+$ cells/mm^3).

(G) Noggin exposure resulted in a reduction in the proportion of SOX2$^+$ cells undergoing cell division.

(H) The number of CldU$^+$LRCs that were still proliferating (incorporated IdU) was diminished. Unpaired Student's t test: *$p < 0.05$, **$p < 0.01$. See also Figure S6 for additional data.

Figure 5F), whereas the proportion of proliferating nonradial cells (Figure 5F) or DCX$^+$ neuroblasts remained constant (percentage of DCX$^+$ cells that were BrdU$^+$: 5.4% ± 0.7% in saline versus 6.9 ± 2.6% in Noggin, $p = 0.3$, Figure 5K). Immunofluorescence analysis with Ki67 further showed that the percentage of cycling radial NSCs increased (Figures 5I and 5J), indicating that the Noggin-mediated attenuation of BMP signaling recruited quiescent (G_0) radial cells into the cycle. In accordance with the increase in NSC division, hippocampal neurogenesis was augmented upon Noggin administration, as scored by the number of DCX$^+$ immature neurons ($p < 0.001$, Figure 5L).

Blockade of BMP Signaling Leads to a Decrease in Proliferation and to the Loss of SOX2$^+$ Nonradial Cells

In another set of animals, Noggin infusion was combined with the administration of two halogenated thymidine analogs to label and distinguish proliferating cells at different time points (Figure 6A). Noggin was administered over 1 week, and 5-clorodeoxyuridine (CldU) was injected on the last day of infusion (day 7). Next, the catheter connecting the pump to the cannula was sealed, and animals were returned to the cages for 3 additional weeks. Prior to euthanasia, animals received 5-iododeoxyuridine (IdU), which allowed us to discriminate between CldU$^+$ label-retaining stem cells (LRCs) that remained in the SGZ after the proliferative burst triggered by Noggin and IdU$^+$ cells that were dividing 28 days after they were first exposed to the BMP antagonist.

At least two major classes of cells in the hippocampal dentate gyrus were expected to retain the CldU label: slowly dividing SOX2$^+$ NSCs that do not dilute CldU through division (LRCs) and newborn neurons that incorporate CldU prior to cell cycle exit. As shown in Figure 6B, the number of SOX2$^+$CldU$^+$ LRCs per mm^3 in the SGZ was significantly reduced in brains that had been exposed to Noggin (619 ± 209 in saline [n = 5] versus 342 ± 124 in Noggin [n = 3], $p < 0.05$). Conversely, Noggin infusion significantly increased the number of CldU$^+$ cells that had matured to granule neurons ($p < 0.05$, Figure 6C). Among the cells that retained CldU, the proportion of SOX2$^+$ undifferentiated cells and that of their differentiated progeny (immature DCX$^+$ neurons or more mature NeuN$^+$ neurons) were shifted after Noggin infusion in favor of the differentiated phenotypes (Figure 6D).

In Noggin-treated animals, we observed that total SOX2$^+$ cell numbers were diminished because of a reduction in SOX2$^+$ nonradial cells ($p < 0.01$, Figure 6E). Accordingly, and as measured by anti-IdU immunostaining, overall proliferation in the SGZ was also diminished ($p < 0.05$, Figure 6F). The percentage of the SOX2$^+$ cell population that was in S-phase declined ($p < 0.05$, Figure 6G), the birth of new IdU$^+$DCX$^+$ neurons showed a marked tendency toward reduction (double-positive cells per mm^3: 4446 ± 729 in saline versus 2596 ± 702 in Noggin, $p = 0.09$), and the total number of DCX$^+$ cells per mm^3 was significantly diminished (21417 ± 2844 in saline versus 14785 ± 4134 in Noggin, $p < 0.05$). Of note, the number of double-labeled CldU$^+$IdU$^+$ cells in the SGZ decreased in the Noggin group compared to the saline condition ($p < 0.05$, Figure 6H), pointing to a restriction in the proliferative activity of LRCs.

To test the possibility that the loss of nonradial SOX2$^+$ cells was due to cell death, we examined the hippocampus at intermediate time points after Noggin infusion (Figure S6). Despite the progressive decline in the number of SOX2$^+$ nonradial cells, we could not detect any increase in the number of cleaved Caspase 3$^+$ nuclei in the SGZ. Thus, the cellular loss among the SOX2$^+$ nonradial pool was probably due to a decreased production of SOX2$^+$ nonradial cells but not to enhanced cell death.

BMPR-IA and Smad4 Are Required for Maintaining AH-NSC Activity and Neurogenesis In Vivo

We next designed a cell type- and time-specific strategy to accurately examine the role of canonical BMP signaling downstream of BMPR-IA in the regulation of AH-NSCs. We developed a lentivirus (LV)-mediated knockout technique to selectively delete *Bmpr1a* in *Sox2*-expressing cells (Figure 7A). *Bmpr1a*$^{flox/null}$ mice were stereotactically injected into the dentate gyrus with a LV expressing Cre recombinase fused to GFP under the regulation of the *Sox2* promoter (LV-*Sox2*-CreGFP). As a control, *Bmpr1a*$^{flox/wt}$ and *Bmpr1a*$^{flox/null}$ mice were injected with LV-*Sox2*-CreGFP or LV-*Sox2*-GFP, respectively. Animals received BrdU either 10 days or 4 weeks after LV injection. Among the LV-infected cells (GFP$^+$), the percentage of P-SMAD1$^+$ cells declined from 74.6% ± 5.7% (average ± SEM) in control mice to 38.5% ± 7.7% in *Bmpr1a*$^{flox/null}$ *mice*, indicating that canonical signaling was impaired. Ten days after *Bmpr1a* deletion, proliferation was increased in the SGZ, although high experimental variability and a local inflammatory response were observed. To analyze long-term effects of conditional *Bmpr1a* deletion in NSCs, we examined animals 28 days after LV injection. At this late time point, proliferation was markedly decreased (57% reduction, $p < 0.05$, Figures 7C and 7D), which is in accordance to our previous observations. Consistent with this finding, the total number of SGZ SOX2$^+$ cells was 51% lower ($p < 0.05$, Figures 7D and 7E), and the number of DCX$^+$ immature neurons was strongly reduced ($p < 0.05$, Figures 7D and 7F), indicating that neurogenesis was severely impaired upon deletion of *Bmpr1a*.

We next used a genetic approach to conditionally delete *Smad4*, a central player of the canonical BMP pathway, in the radial NSC population. We took advantage of the *GLAST:CreERT2* mouse line that expresses the tamoxifen-inducible form of Cre in adult NSCs (Ninkovic et al., 2007). *GLAST:CreERT2* animals were crossed with the *Smad4*$^{flox/flox}$ mouse line, and after tamoxifen-induced deletion of *Smad4*, dividing cells were labeled by means of BrdU. Animals were examined either immediately after or 3 weeks later (Figure 7G). We observed an increase in BrdU incorporation in the SGZ of conditionally deleted *Smad4* mice that were analyzed at short time points (BrdU$^+$ cells per mm^3: 751 ± 213 in *Smad4*$^{wt/wt}$ *versus* 1733 ± 47 in *Smad4*$^{flox/flox}$, $p < 0.05$, Figure 7H), yet when mice were examined 3 weeks later, we observed a reduction in SOX2$^+$ cell numbers, which was attributed to a decrease in non-radial cells (Figures 7I and 7J). This finding is in accordance with our previous data and clearly indicates that *Bmpr1a* and *Smad4* are involved in regulating the activity and the number of stem/precursor cells in the adult SGZ.

Our results demonstrate that canonical BMP signaling downstream of the BMP type IA receptor plays a key role in vivo in regulating quiescence of radial NSCs, which is required to maintain the proliferative capacity of the hippocampal stem cell pool and thus to support continuous neurogenesis throughout the adult life.

DISCUSSION

Interactions between neurogenic niches and NSCs play a critical role in the homeostatic regulation of adult neurogenesis. Signaling from the niche is proposed to control many aspects of NSC behavior, such as balancing the quiescent and proliferative status of NSCs (in order to regulate the rate of neurogenesis), determining the cell division mode (symmetric versus asymmetric, to preserve the NSC pool), and preventing premature depletion of stem cells, or the loss of their properties, to maintain neurogenesis throughout life (Morrison and Spradling, 2008; Miller and Gauthier-Fisher, 2009). Disrupted homeostatic influence of neurogenic niches onto NSCs can promote pathological conditions such as cellular aging and tumorigenesis (Voog and Jones, 2010). Thus, identifying and understanding niche signals can shed light on how adult neurogenesis is regulated and can provide a key to successful NSC-mediated regenerative medicine.

Here, we have addressed the function of BMP signaling in the hippocampal stem cell niche from fully mature mice by combining in vitro experiments, brain infusion of the antagonist Noggin, label-retaining assays, and conditional inactivation of *Bmpr1a* or *Smad4* in stem cells. On the basis of our findings, we propose that BMPs participate as dominant niche signals in the adult hippocampus to restrict proliferation of the stem cell pool. All our studies supported this notion, demonstrating that (1) BMP canonical signaling is active in the majority of the SOX2$^+$ cell population in the hippocampus, which is predominantly out of the cell cycle (Suh et al., 2007), including the BMPRI-A$^+$ radial stem cell pool; (2) BMP canonical signaling is blocked in SOX2$^+$ cells that actively proliferate and incorporate BrdU; (3) BMPs reversibly counteract the mitogenic stimulation of cultured SOX2$^+$ AH-NSCs, driving the cells into quiescence; and (4) downregulation of endogenous BMP signaling increases proliferation of SOX2$^+$ cells in the hippocampus by recruiting quiescent (G_0) radial cells into the cycle and consequently leads to enhanced neurogenesis. Thus, the ultimate role of BMPs in the adult hippocampal niche is to govern the balance between the quiescent and proliferative state of NSCs, thereby modulating stem cell activity and neurogenesis in the SGZ. These results consolidate BMP ligands and BMPR-IA signaling as widespread regulators of stem cell division in a variety of adult somatic niches (Varga and Wrana, 2005; Morrison and Spradling, 2008). In addition, we have also found that canonical signaling becomes reactivated in the hippocampus shortly after neuronal fate commitment, possibly implicating the BMPR-IB receptor in the maturation and/or cell cycle exit of newly born neurons (Figure S7).

Our studies also provided a mechanistic understanding of how BMPs transduce signals into NSCs. BMPR-IA is responsible for triggering the canonical BMP pathway by phosphorylating the SMAD1 protein. Using both adherent and neurosphere stem cell cultures, we have found that the canonical BMP pathway primarily acts to restrict AH-NSC division in the presence of a mitogenic stimulus without affecting stem cell identity. The decrease in proliferation is due, at least in part, to an increase in the proportion of cells that enters quiescence. The effect is reversible and proliferation is resumed once the culture is depleted of BMP. Moreover, translocation of P-SMAD1 is associated with the upregulation of target genes, such as *Id1-4* and *Hes1*. All the aforementioned genes are known to block the action of prodifferentiation bHLH factors in the developing ventricular zone of the central nervous system (Ishibashi et al., 1994; Nakashima et al., 2001; Ohtsuka et al., 2001; Hatakeyama

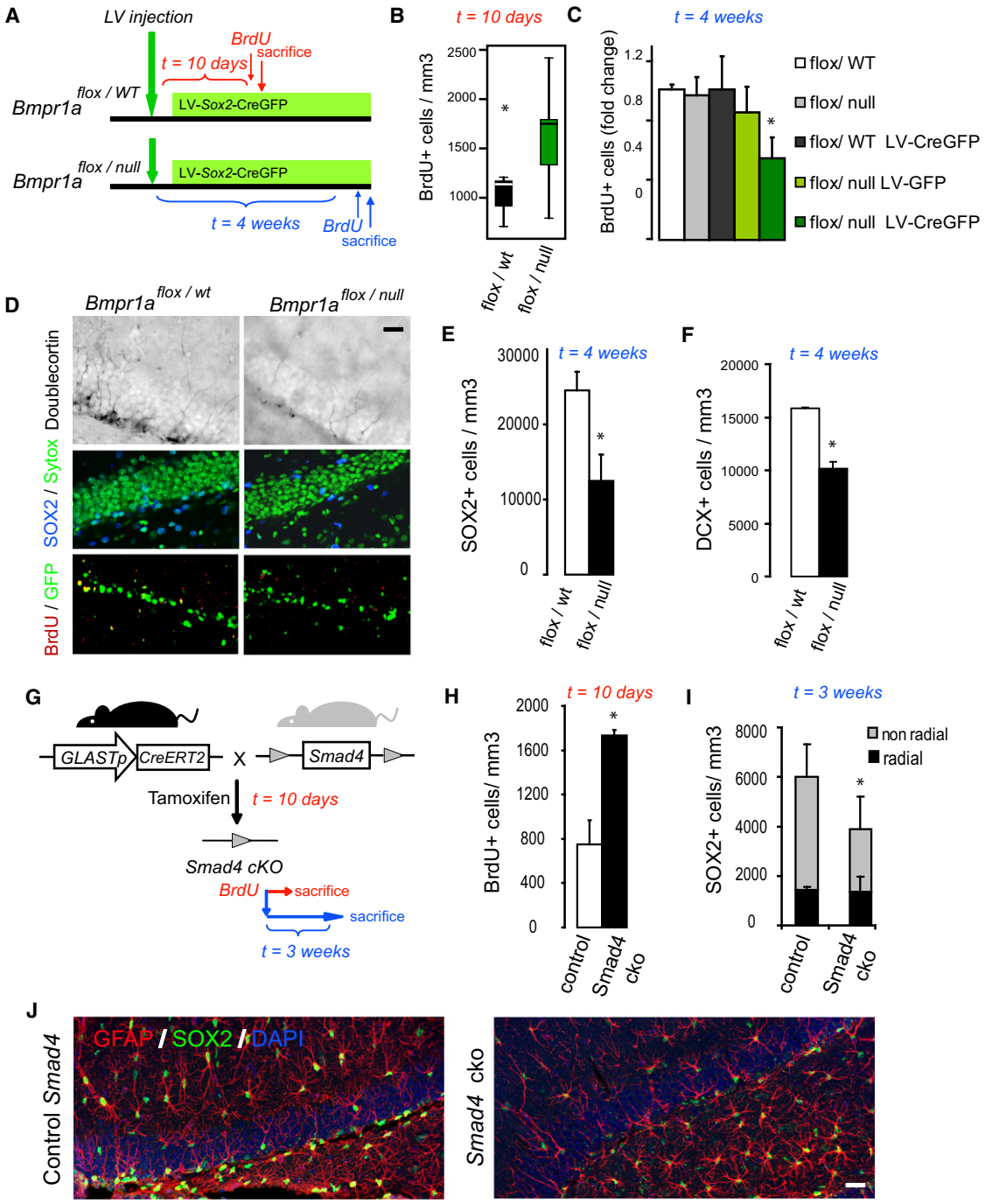

Figure 7. Conditional Ablation of *Bmpr1a* or *Smad4* Compromises Stem Cell Maintenance and Neurogenesis

(A) Scheme illustrating the LV-based strategy for selective deletion of the *Bmpr1a* allele in *Sox2*-expressing cells. BrdU was administered prior to sacrifice, either 10 days or 4 weeks after LV injection.

(B) Box and whiskers plot showing that median proliferation is increased in $Bmpr1a^{flox/null}$ mice injected with the LV expressing GFP/Cre fusion in $SOX2^+$ cells after 10 days. Note the dispersion of the data at this early time point (Mann-Whitney U-test, $p < 0.05$).

(C) Proliferation is significantly decreased in $Bmpr1a^{flox/null}$ mice injected with the LV expressing GFP/Cre after 4 weeks. No change was observed in noninjected contralateral hemispheres (control) or in $Bmpr1a^{flox/null}$ mice injected with the LV expressing GFP.

(D) Immunohistochemical analysis of $Bmpr1a^{flox/null}$ and $Bmpr1a^{flox/wt}$ mice injected with the LV expressing GFP/Cre after 4 weeks. The number of proliferating cells (bottom, $BrdU^+$, red), the number of stem/precursor cells (middle, $SOX2^+$, blue), and the number of new neurons (top, DCX^+, gray) were reduced. SGZ LV-infected cells expressing GFP (green) are shown in the bottom panel.

(E) Quantitative analysis of $Bmpr1a^{flox/null}$ and $Bmpr1a^{flox/wt}$ mice injected with the LV expressing GFP/Cre demonstrates the depletion in $SOX2^+$ cells.

(F) The reduction in the number of DCX^+ neurons observed in (D).

et al., 2004). Induction of the *Hes1* gene is particularly interesting because HES1 can act as a safeguard against irreversible cell cycle exit during quiescence, thereby possibly preventing premature senescence and inappropriate differentiation of AH-NSCs (Sang et al., 2008). As opposed to the BMP treatment, the addition of the antagonist Noggin to neurosphere cultures increased the number of spheres, their diameter, and the percentage of cells per sphere that were in the cell cycle, indicating that AH-NSCs secrete BMPs, which may act to regulate proliferation in an autocrine manner.

A relevant aspect of our in vivo results is that although blockade of BMP signaling in the hippocampus first stimulates proliferation, it leads subsequently to the loss of the regenerative capacity of the radial stem cell population. The early impact of Noggin infusion is an increase in proliferation, but the consequence after 3 weeks is a reduction in proliferation and a depletion of newborn neurons (which were also detected in *Smad4*- and *Bmpr1a*-deleted animals). Importantly, by consecutively labeling cells with CldU and IdU, we observed that $CldU^+IdU^+$ double-positive cells in the SGZ were diminished 4 weeks after the onset of Noggin infusion, pointing to a restriction in the proliferative activity of the LRCs that were challenged to divide earlier. This finding differs from a recent report showing that continuous Noggin release from neuronal cells increases the number of slowly dividing LRCs (Bonaguidi et al., 2008). However, in that study, the interval between the administration of the two thymidine analogs was shorter, perhaps explaining their different results. Alternatively, it is possible that acute delivery of Noggin by pump infusion may have caused a response that differs from the effect triggered by a continuous Noggin release. Interestingly, we also observed that 4 weeks after blocking the BMP pathway, the number of nonradial $SOX2^+$ cells was reduced, whereas the number of $SOX2^+$ $GFAP^+$ radial cells remained constant. This observation is compatible with a model in which the production of nonradial cells by adult hippocampal radial NSCs in vivo becomes compromised after a certain number of mitotic rounds, resembling the behavior of NSCs in the aged hippocampus (Hattiangady and Shetty, 2008; Aizawa et al., 2009). In conclusion, our interpretation of the data presented herein is that a prolonged blockade of the BMP pathway can lead to a premature loss in the ability of activated hippocampal stem cells to proliferate and generate progeny in vivo. However, at later time points, feedback mechanisms elicited by the decline in stem cell activity could recruit a backup of dormant NSCs to replenish the niche.

Together, our findings reveal an aspect of BMP signaling in adult NSC niches, as a master regulator of quiescence, and may provide a key to understanding the maintenance of neurogenesis in the adult hippocampus. At the same time, our studies raise several questions regarding BMP function. First, it is tempting to speculate that the effects of diverse neurogenic external stimuli, such as learning, voluntary exercise, enriched environment, or treatment with antidepressant drugs (reviewed by Ming and Song, 2005; Zhao et al., 2008), may converge mechanistically on an increase in inhibitory factors that block BMP signaling. In support of this view, it has been reported that running increases *Noggin* expression and decreases *Bmp4* expression in hippocampal tissue, and the resulting blockade of BMP signaling is crucial for the effects of exercise on neurogenesis and cognition in mice (Gobeske et al., 2009). In contrast, it has been shown that decreased neurogenesis in a transgenic mouse model of Alzheimer's disease is accompanied by increased expression of *Bmp4* and decreased expression of *Noggin* (Tang et al., 2009), pointing to a broad role for the niche's balance of BMP antagonists/ligands in controlling adult NSCs. However, the identification of the cellular source of BMP ligands and antagonists in vivo needs to be investigated further. Second, as shown in our in vitro studies, BMPs counteract mitogenic signals such as FGF2; thus, understanding the interplay between the BMP pathway and other signaling pathways may be crucial to unraveling how adult NSC division is balanced. Among the endogenous molecules that are expressed in the dentate gyrus of rodents and that have been shown to regulate hippocampal NSCs, Shh (Favaro et al., 2009) and Wnt3 (Lie et al., 2005) may be relevant (Figure S7). Given the antagonistic function of BMP and Shh in mediating the development of some central nervous system structures, and given the role of the fine-tuned activity of the BMP and Wnt pathways in the switch from stem cell quiescence to active proliferation in several adult organs (reviewed by Li and Clevers, 2010), future attempts should be made to understand the function of BMP signaling in a context-dependent manner.

EXPERIMENTAL PROCEDURES

Cell Culture

For proliferation and electroporation assays, AH-NSCs were grown as described in Supplemental Experimental Procedures. Recombinant BMP2/BMP4 (R&D Systems) and Noggin (Sigma) were added at the indicated concentrations.

Immunostaining

Tissue and cultured cells were fixed with 4% paraformaldehyde and processed for immunostaining. Primary and secondary antibodies employed are listed in Supplemental Experimental Procedures. Stained specimens were analyzed with either a Bio-Rad Radiance confocal imaging system (Hercules, CA), a Leica TCS-SL spectral confocal (Heidelberg, Germany), or a Nikon Eclipse 800 microscope (Nikon, Melville, NY).

Flow Cytometry

Analysis was performed on Hoechst 33342 (Sigma) and Pyronin Y (Sigma) stained cells with a FACSVantage cytometer (Becton Dickinson), as described in Supplemental Experimental Procedures. Oregon Green 488 carboxylic acid diacetate succimidyl ester (DFFDA, Molecular Probes) was used for staining neurospheres. $DFFDA^{high}$ cells were sorted in FACSAria (Becton Dickinson) equipment.

(G) Diagram illustrating the experimental design employed for the selective deletion of *Smad4* in GLAST-expressing adult radial stem cells. BrdU was injected 10 days after the administration of tamoxifen. Animals were either sacrificed immediately after or 3 weeks later.
(H) Soon after tamoxifen treatment, proliferation in the SGZ of *Smad4* conditional knockouts was increased.
(I and J) Three weeks later, the number of nonradial precursors diminished but the number of radial NSCs remained unchanged. The confocal image shows the maximal projection of a 17-micron stack. GFAP staining is shown in red, SOX2 is shown in green, and DAPI is shown in blue. Unpaired Student's t test: $*p < 0.05$. The scale bar represents 40 μm.

Intracerebroventricular Infusion

Infusion was performed using Alzet osmotic mini-pumps (see Supplemental Experimental Procedures for additional details). In one experimental paradigm, animals were injected intraperitoneally with 50 mg BrdU/kg of body weight (seven times, once every 2 hours) on the last day of infusion and were sacrificed 1 hr after the last injection. In a second experimental paradigm, CldU (42.5 mg/kg) was injected on the last day of infusion (three times every 2 hr). Next, the catheter connecting the pump to the cannula was sealed. After 3 additional weeks, animals received IdU (57.5 mg/kg) over 3 days (six times every 12 hr) and were sacrificed 12 hr after the last injection. Handling of mice was carried out in accordance with 86/609/EEC guidelines. The animal procedures were performed in accordance with protocols approved by the Instituto de Salud Carlos III animal care and use committee.

Lentiviral Vectors and In Vivo Injections

Lentiviral vectors expressed either GFP or GFP/Cre fusion protein under the control of *Sox2* promoter. A total of 1.5 μl of the viral concentrate was stereotactically injected into the right hippocampal dentate gyrus (see Supplemental Experimental Procedures for additional details). Ten days post-surgery, animals were injected intraperitoneally with BrdU four times at 2 hr intervals and were sacrificed two hours after the last injection. A separate group of animals was injected with BrdU four weeks post-surgery, once daily for three consecutive days, at a dose of 100 mg/kg body weight. Animals were perfused 24 hr after the final BrdU injection. All animal procedures were performed according to protocols approved by The Salk Institute for Biological Studies animal care and use committee.

SUPPLEMENTAL INFORMATION

Supplemental Information includes Supplemental Experimental Procedures and seven figures and can be found with this article online at doi:10.1016/j.stem.2010.04.016.

ACKNOWLEDGMENTS

The authors thank Dr.Yuji Mishina for *Bmpr1a*$^{flox/flox}$ and *Bmpr1a*$^{wt/null}$ mice and Dr. C.X. Deng for the *Smad4*$^{flox/flox}$ mice. They also thank Mary Lynn Gage for editorial support, Dr. Pilar Sánchez-Gómez for helpful discussions and suggestions, Dr. Mari Paz Rubio, Maria José Palop, André Luis Carvalho, Mireia Moreno, Yolanda Noriega, and Mario Alía for technical assistance. S.J. was supported in part by the Deutsche Forschungsgemeinschaft; H.M. was supported by the Programa Ramon y Cajal from the Spanish Ministerio de Educacion y Ciencia (MEC); Z.A. was supported by the Centro de Investigación Príncipe Felipe; and M.A.M-T. is a recipient of a pre-doctoral fellowship from the FPI/MEC. M.G. was funded by Helma and SFB 596. Additional support was provided by grants from Ministerio de Sanidad y Consumo (MSC; Fondo de Investigación Sanitaria-PI06/0754 and PI09/2254) to H.M.; from MEC (SAF2005-06325), MSC (RETIC Tercel and CIBERNED) and Fundación "la Caixa" to I.F., and from the Bavarian Network on Adult Neural Stem Cells "FORNEUROCELL" to D.C.L.

Received: October 3, 2008
Revised: November 13, 2009
Accepted: April 13, 2010
Published: July 1, 2010

REFERENCES

Aizawa, K., Ageyama, N., Terao, K., and Hisatsune, T. (2009). Primate-specific alterations in neural stem/progenitor cells in the aged hippocampus. Neurobiol. Aging, in press. Published online February 6, 2009. 10.1016/j.neurobiolaging.2008.12.011.

Bonaguidi, M.A., Peng, C.Y., McGuire, T., Falciglia, G., Gobeske, K.T., Czeisler, C., and Kessler, J.A. (2008). Noggin expands neural stem cells in the adult hippocampus. J. Neurosci. *28*, 9194–9204.

Charytoniuk, D.A., Traiffort, E., Pinard, E., Issertial, O., Seylaz, J., and Ruat, M. (2000). Distribution of bone morphogenetic protein and bone morphogenetic protein receptor transcripts in the rodent nervous system and up-regulation of bone morphogenetic protein receptor type II in hippocampal dentate gyrus in a rat model of global cerebral ischemia. Neuroscience *100*, 33–43.

Chen, H.L., and Panchision, D.M. (2007). Concise review: Bone morphogenetic protein pleiotropism in neural stem cells and their derivatives—alternative pathways, convergent signals. Stem Cells *25*, 63–68.

Cheng, T., Rodrigues, N., Shen, H., Yang, Y., Dombkowski, D., Sykes, M., and Scadden, D.T. (2000). Hematopoietic stem cell quiescence maintained by p21cip1/waf1. Science *287*, 1804–1808.

Colak, D., Mori, T., Brill, M.S., Pfeifer, A., Falk, S., Deng, C., Monteiro, R., Mummery, C., Sommer, L., and Götz, M. (2008). Adult neurogenesis requires Smad4-mediated bone morphogenic protein signaling in stem cells. J. Neurosci. *28*, 434–446.

Coskun, V., Venkatraman, G., Yang, H., Rao, M.S., and Luskin, M.B. (2001). Retroviral manipulation of the expression of bone morphogenetic protein receptor Ia by SVZa progenitor cells leads to changes in their p19(INK4d) expression but not in their neuronal commitment. Int. J. Dev. Neurosci. *19*, 219–227.

Favaro, R., Valotta, M., Ferri, A.L., Latorre, E., Mariani, J., Giachino, C., Lancini, C., Tosetti, V., Ottolenghi, S., Taylor, V., and Nicolis, S.K. (2009). Hippocampal development and neural stem cell maintenance require Sox2-dependent regulation of Shh. Nat. Neurosci. *12*, 1248–1256.

Filippov, V., Kronenberg, G., Pivneva, T., Reuter, K., Steiner, B., Wang, L.P., Yamaguchi, M., Kettenmann, H., and Kempermann, G. (2003). Subpopulation of nestin-expressing progenitor cells in the adult murine hippocampus shows electrophysiological and morphological characteristics of astrocytes. Mol. Cell. Neurosci. *23*, 373–382.

Fukuda, S., Kato, F., Tozuka, Y., Yamaguchi, M., Miyamoto, Y., and Hisatsune, T. (2003). Two distinct subpopulations of nestin-positive cells in adult mouse dentate gyrus. J. Neurosci. *23*, 9357–9366.

Gobeske, K.T., Das, S., Bonaguidi, M.A., Weiss, C., Radulovic, J., Disterhoft, J.F., and Kessler, J.A. (2009). BMP signaling mediates effects of exercise on hippocampal neurogenesis and cognition in mice. PLoS ONE *4*, e7506.

Hall, A.K., and Miller, R.H. (2004). Emerging roles for bone morphogenetic proteins in central nervous system glial biology. J. Neurosci. Res. *76*, 1–8.

Hatakeyama, J., Bessho, Y., Katoh, K., Ookawara, S., Fujioka, M., Guillemot, F., and Kageyama, R. (2004). Hes genes regulate size, shape and histogenesis of the nervous system by control of the timing of neural stem cell differentiation. Development *131*, 5539–5550.

Hattiangady, B., and Shetty, A.K. (2008). Aging does not alter the number or phenotype of putative stem/progenitor cells in the neurogenic region of the hippocampus. Neurobiol. Aging *29*, 129–147.

Ishibashi, M., Moriyoshi, K., Sasai, Y., Shiota, K., Nakanishi, S., and Kageyama, R. (1994). Persistent expression of helix-loop-helix factor HES-1 prevents mammalian neural differentiation in the central nervous system. EMBO J. *13*, 1799–1805.

Kippin, T.E., Martens, D.J., and van der Kooy, D. (2005). p21 loss compromises the relative quiescence of forebrain stem cell proliferation leading to exhaustion of their proliferation capacity. Genes Dev. *19*, 756–767.

Kronenberg, G., Reuter, K., Steiner, B., Brandt, M.D., Jessberger, S., Yamaguchi, M., and Kempermann, G. (2003). Subpopulations of proliferating cells of the adult hippocampus respond differently to physiologic neurogenic stimuli. J. Comp. Neurol. *467*, 455–463.

Li, L., and Clevers, H. (2010). Coexistence of quiescent and active adult stem cells in mammals. Science *327*, 542–545.

Lie, D.C., Colamarino, S.A., Song, H.J., Désiré, L., Mira, H., Consiglio, A., Lein, E.S., Jessberger, S., Lansford, H., Dearie, A.R., and Gage, F.H. (2005). Wnt signalling regulates adult hippocampal neurogenesis. Nature *437*, 1370–1375.

Lim, D.A., Tramontin, A.D., Trevejo, J.M., Herrera, D.G., García-Verdugo, J.M., and Alvarez-Buylla, A. (2000). Noggin antagonizes BMP signaling to create a niche for adult neurogenesis. Neuron *28*, 713–726.

Miller, F.D., and Gauthier-Fisher, A. (2009). Home at last: Neural stem cell niches defined. Cell Stem Cell *4*, 507–510.

Ming, G.L., and Song, H. (2005). Adult neurogenesis in the mammalian central nervous system. Annu. Rev. Neurosci. *28*, 223–250.

Morrison, S.J., and Spradling, A.C. (2008). Stem cells and niches: Mechanisms that promote stem cell maintenance throughout life. Cell *132*, 598–611.

Nakashima, K., Takizawa, T., Ochiai, W., Yanagisawa, M., Hisatsune, T., Nakafuku, M., Miyazono, K., Kishimoto, T., Kageyama, R., and Taga, T. (2001). BMP2-mediated alteration in the developmental pathway of fetal mouse brain cells from neurogenesis to astrocytogenesis. Proc. Natl. Acad. Sci. USA *98*, 5868–5873.

Ninkovic, J., Mori, T., and Götz, M. (2007). Distinct modes of neuron addition in adult mouse neurogenesis. J. Neurosci. *27*, 10906–10911.

Ohtsuka, T., Sakamoto, M., Guillemot, F., and Kageyama, R.J. (2001). Roles of the basic helix-loop-helix genes Hes1 and Hes5 in expansion of neural stem cells of the developing brain. J. Biol. Chem. *276*, 30467–30474.

Panchision, D.M., and McKay, R.D. (2002). The control of neural stem cells by morphogenic signals. Curr. Opin. Genet. Dev. *12*, 478–487.

Pera, E.M., Ikeda, A., Eivers, E., and De Robertis, E.M. (2003). Integration of IGF, FGF, and anti-BMP signals via Smad1 phosphorylation in neural induction. Genes Dev. *17*, 3023–3028.

Ruzankina, Y., Pinzon-Guzman, C., Asare, A., Ong, T., Pontano, L., Cotsarelis, G., Zediak, V.P., Velez, M., Bhandoola, A., and Brown, E.J. (2007). Deletion of the developmentally essential gene ATR in adult mice leads to age-related phenotypes and stem cell loss. Cell Stem Cell *1*, 113–126.

Sang, L., Coller, H.A., and Roberts, J.M. (2008). Control of the reversibility of cellular quiescence by the transcriptional repressor HES1. Science *321*, 1095–1100.

Seri, B., García-Verdugo, J.M., McEwen, B.S., and Alvarez-Buylla, A. (2001). Astrocytes give rise to new neurons in the adult mammalian hippocampus. J. Neurosci. *21*, 7153–7160.

Seri, B., García-Verdugo, J.M., Collado-Morente, L., McEwen, B.S., and Alvarez-Buylla, A. (2004). Cell types, lineage, and architecture of the germinal zone in the adult dentate gyrus. J. Comp. Neurol. *478*, 359–378.

Söderström, S., Bengtsson, H., and Ebendal, T. (1996). Expression of serine/threonine kinase receptors including the bone morphogenetic factor type II receptor in the developing and adult rat brain. Cell Tissue Res. *286*, 269–279.

Suh, H., Consiglio, A., Ray, J., Sawai, T., D'Amour, K.A., and Gage, F.H. (2007). In vivo fate analysis reveals the multipotent and self-renewal capacities of Sox2+ neural stem cells in the adult hippocampus. Cell Stem Cell *1*, 515–528.

Tang, J., Song, M., Wang, Y., Fan, X., Xu, H., and Bai, Y. (2009). Noggin and BMP4 co-modulate adult hippocampal neurogenesis in the APP(swe)/PS1(DeltaE9) transgenic mouse model of Alzheimer's disease. Biochem. Biophys. Res. Commun. *385*, 341–345.

Temple, S., and Alvarez-Buylla, A. (1999). Stem cells in the adult mammalian central nervous system. Curr. Opin. Neurobiol. *9*, 135–141.

ten Dijke, P., Yamashita, H., Sampath, T.K., Reddi, A.H., Estevez, M., Riddle, D.L., Ichijo, H., Heldin, C.H., and Miyazono, K. (1994). Identification of type I receptors for osteogenic protein-1 and bone morphogenetic protein-4. J. Biol. Chem. *269*, 16985–16988.

Varga, A.C., and Wrana, J.L. (2005). The disparate role of BMP in stem cell biology. Oncogene *24*, 5713–5721.

Voog, J., and Jones, D.L. (2010). Stem cells and the niche: a dynamic duo. Cell Stem Cell *6*, 103–115.

Zhao, C., Deng, W., and Gage, F.H. (2008). Mechanisms and functional implications of adult neurogenesis. Cell *132*, 645–660.